Supporting Information

Controlled positioning of MOFs in interfacially polymerized thin-film nanocomposites

*Cédric Van Goethem, Rhea Verbeke, Sanne Hermans, Roy Bernstein, Ivo F.J. Vankelecom**

Materials used

ZIF-8 synthesis

$Zn(NO_3)_2.6H_2O$ (Sigma Aldrich, >99%)

2-methylimidazole (Acros Organics, 99%)

N,N-dimethylformamide (DMF) (Acros Organics, >99%)

Methanol (Fisher Chemical, 99.99%)

Ethanol (Fisher Chemical, absolute grade)

Support membrane preparation

Non-woven PE/PP support (Freudenberg, Novatex 2471)

Polysulfone (PSf) (Udel P-1700)

N-methylpyrrolidon (NMP) (Acros Organics, 98%)

Polyamide toplayer formation

Trimesoylchloride (TMC) (Acros Organics, 98%)

m-phenylenediamine (MPD) (Acros Organics, >99%)

n-hexane (Chemlab, >99%)

NaCl filtration

Sodium Chloride (NaCl) (AnalaR Normapur)

MiliQ water (MQ) (>18.2 MΩ.cm at 25°C)

ZIF-8 characterization

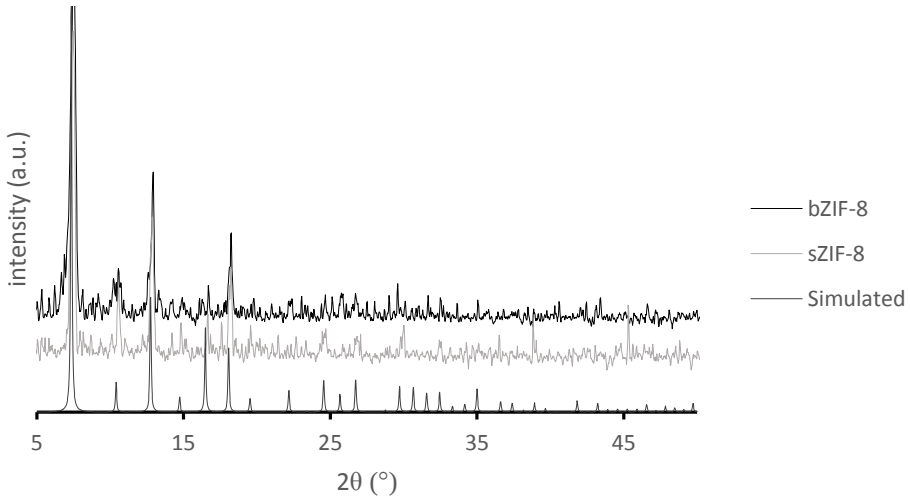

Figure S1: Theoretically predicted X-ray diffraction pattern for ZIF-8 and experimentally obtained diffraction patterns for bZIF and sZIF.

bZIF-EFP-membrane characterization

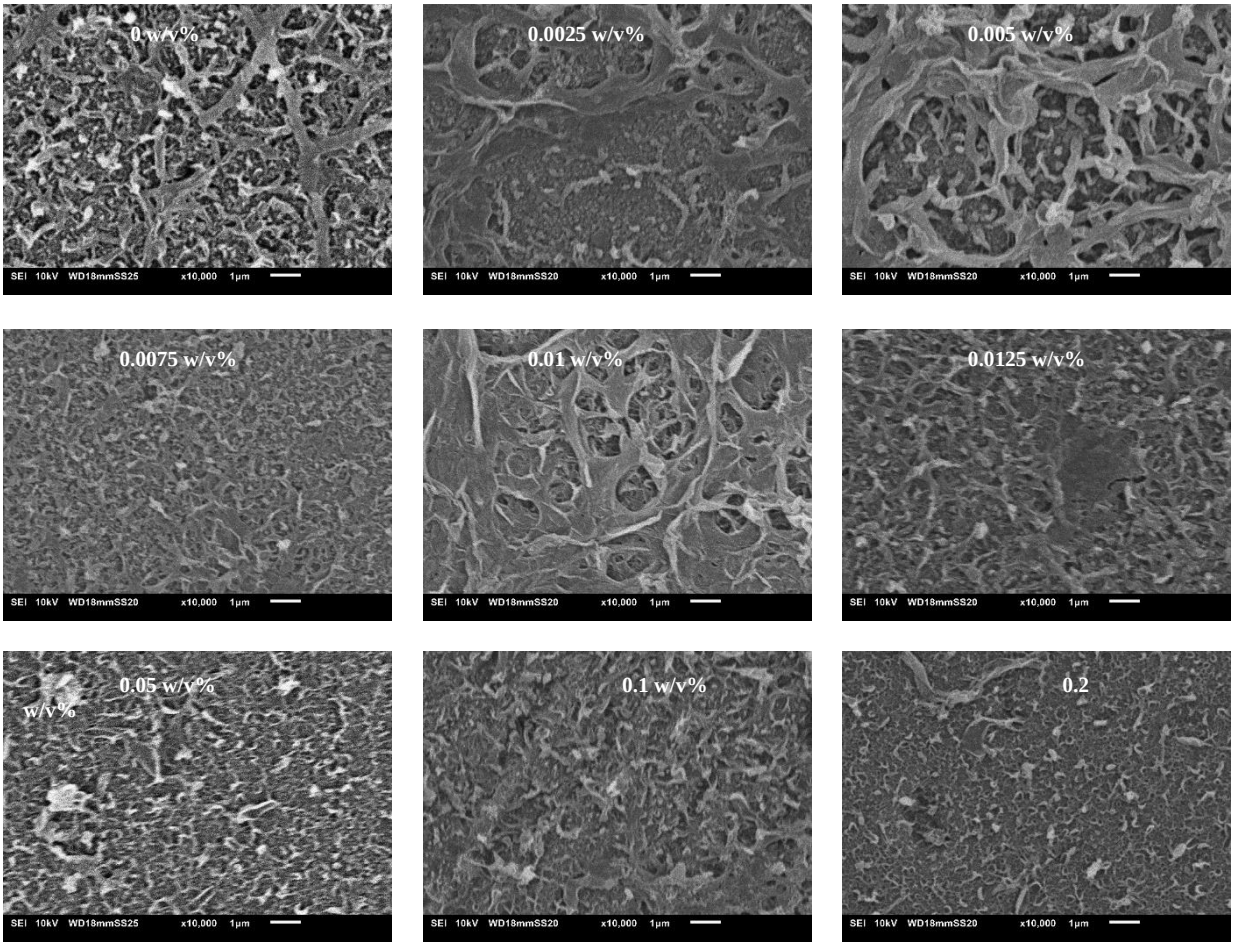

Figure S2: SEM topviews of bZIF-EFP-membranes prepared with different filler concentrations in the hexane solution.

Effect of particle size on EFP-membrane performance

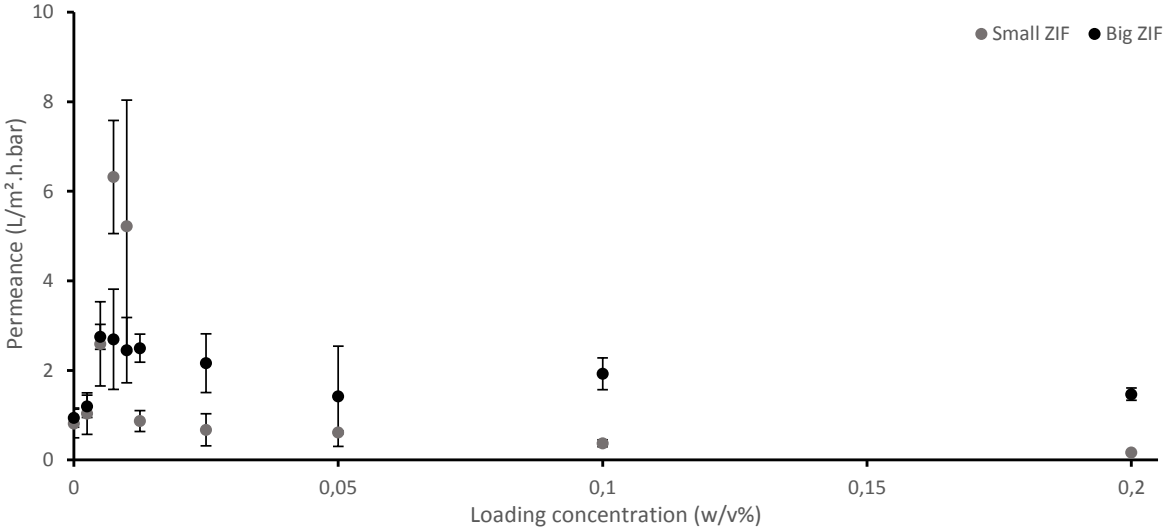

Figure S3: Comparison between the permeability and rejection of bZIF-EFP- and sZIF-EFP-membranes. The permeability of the respective membranes was normalized with respect to the reference membrane of the respective series (sZIF/bZIF).

sZIF-EFP-membrane characterization

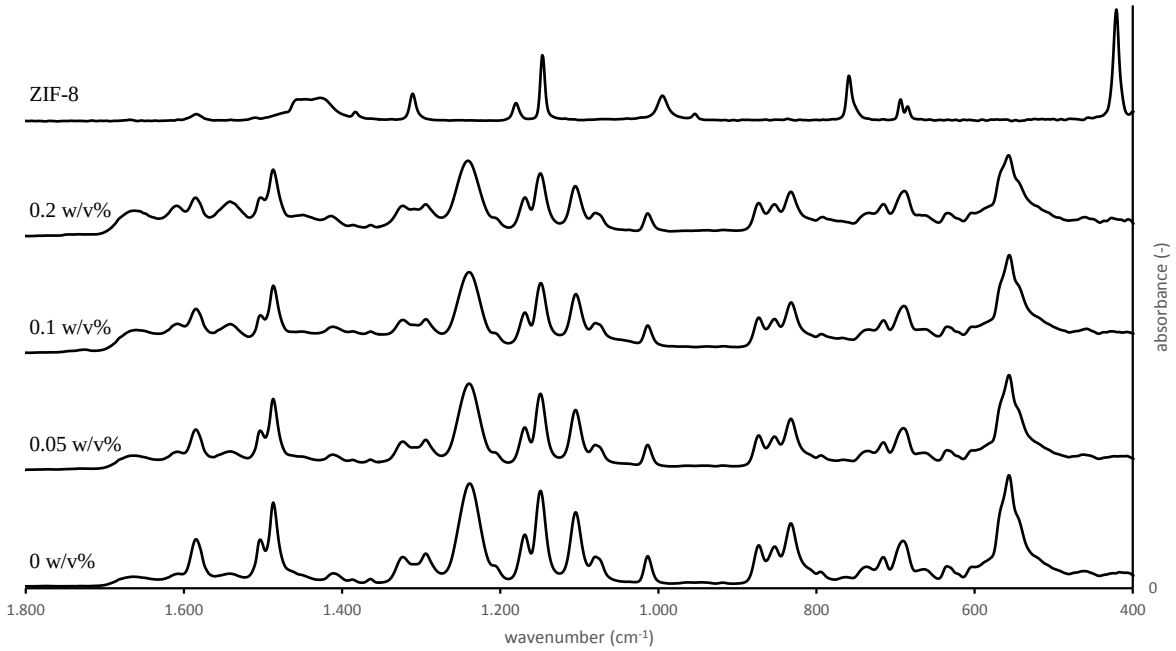

Figure S4: ATR-FTIR absorption spectra of sZIF-EFP-membranes (concentration ZIF-8 used for membrane synthesis is shown in the figure).

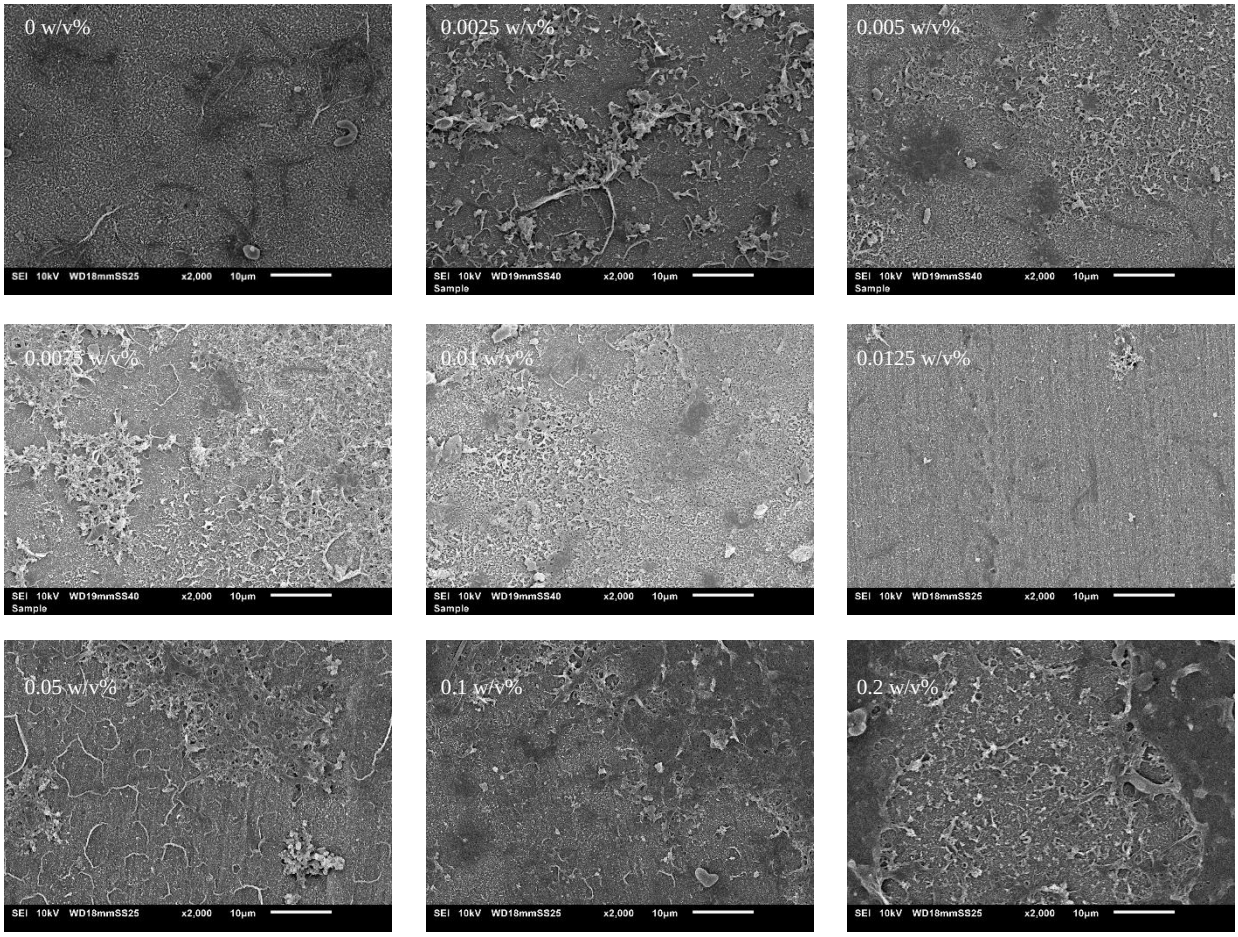

Figure S5: SEM images of the toplayer morphology of sZIF-EFP-membranes with different filler concentration in the hexane solution.

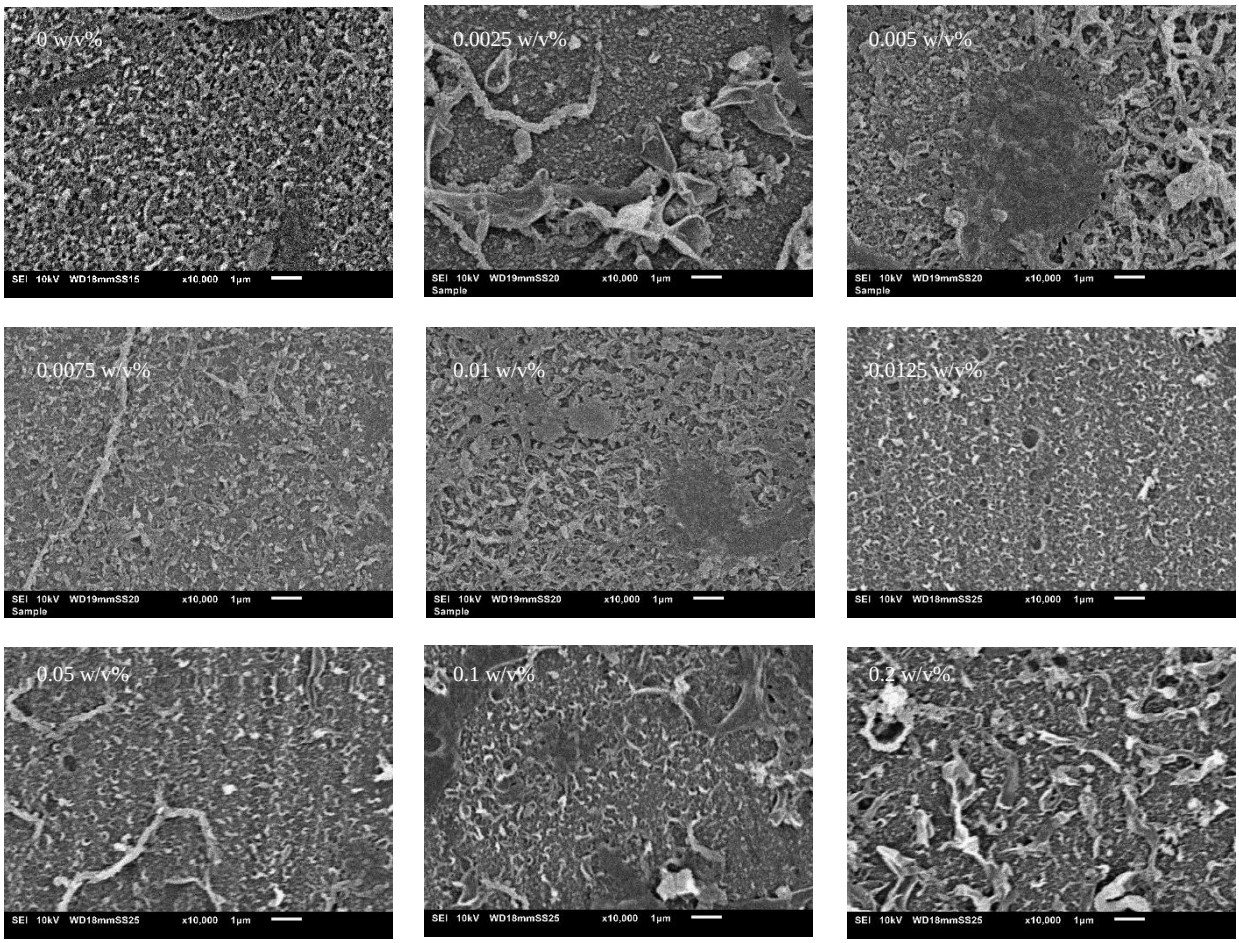

Figure S6: SEM topviews of sZIF-EFP-membranes prepared with different filler concentrations in the hexane solution.

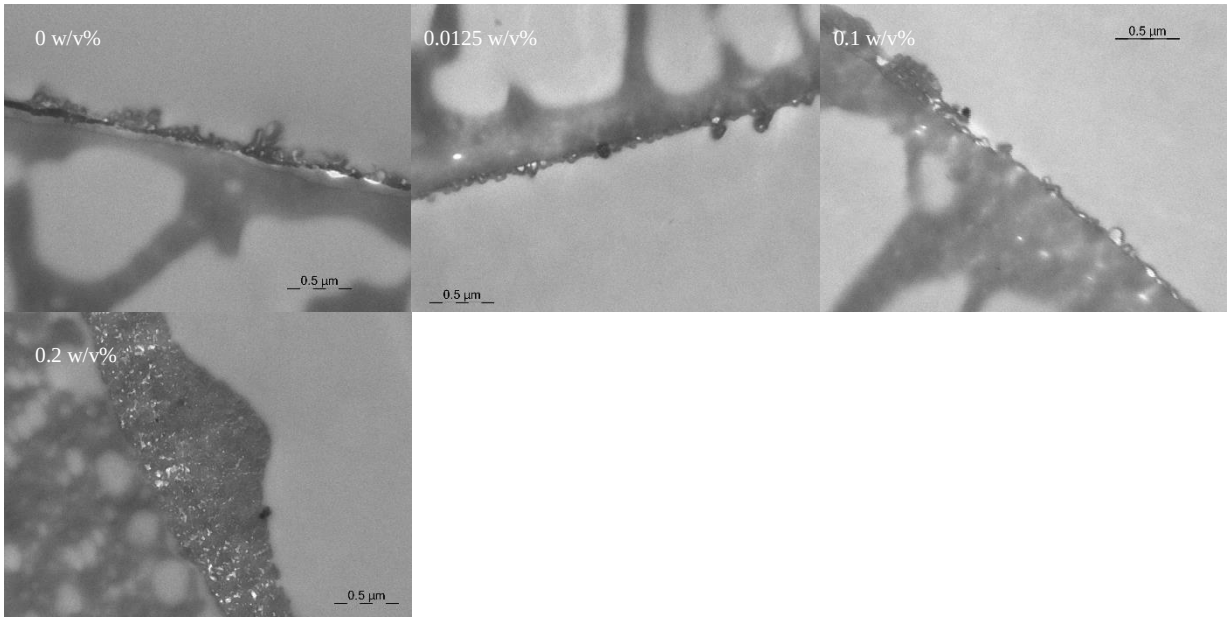

Figure S7: TEM cross-section images of sZIF-EFP-membranes prepared with different filler concentrations in the hexane solution.

CONV-membrane characterization

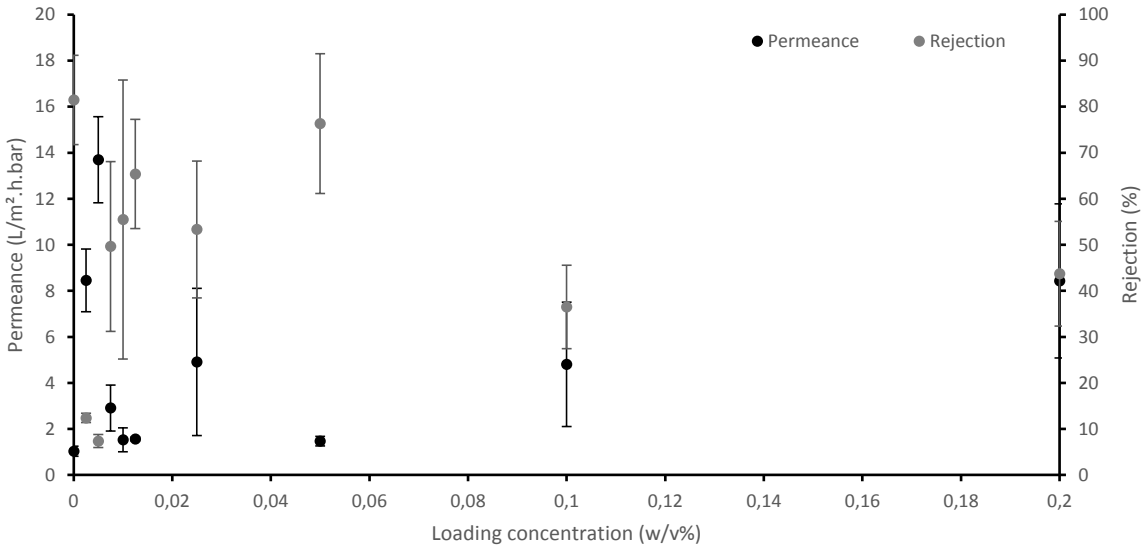

Figure S8: Permeance and rejection of bZIF-CONV-membranes for a 1000 ppm NaCl in MiliQ feed.

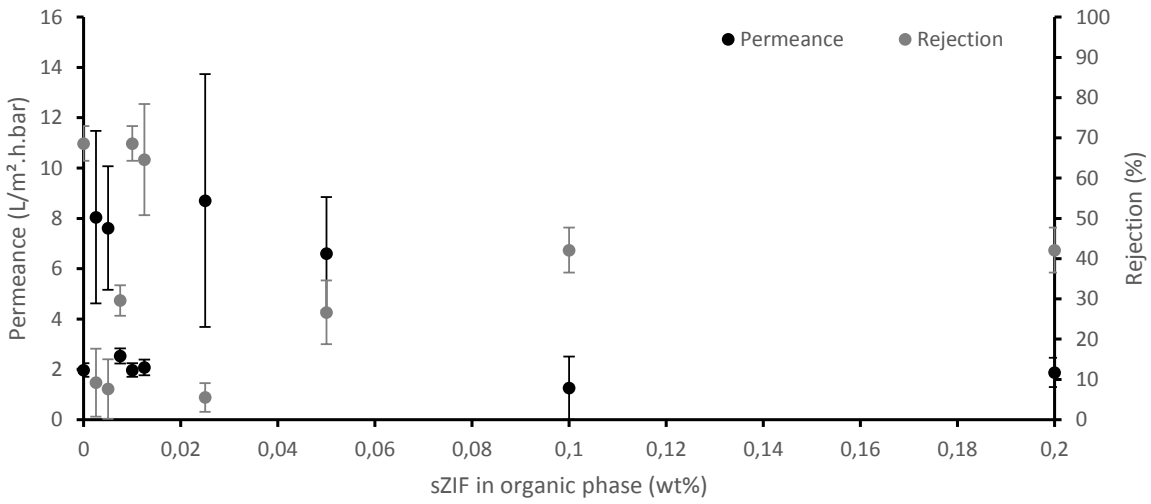

Figure S9: Permeance and rejection of sZIF-CONV-membranes for a 1000 ppm NaCl in MiliQ feed.

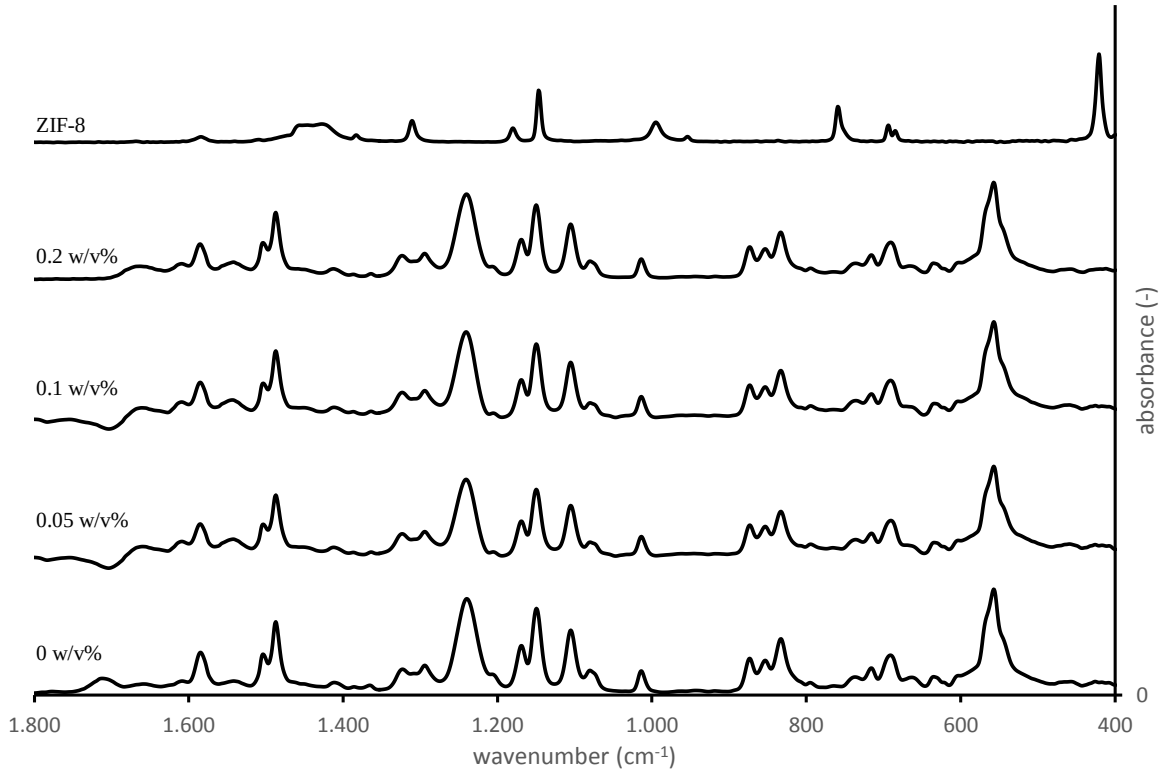

Figure S10: ATR-FTIR absorption spectra of bZIF-CONV-membranes.

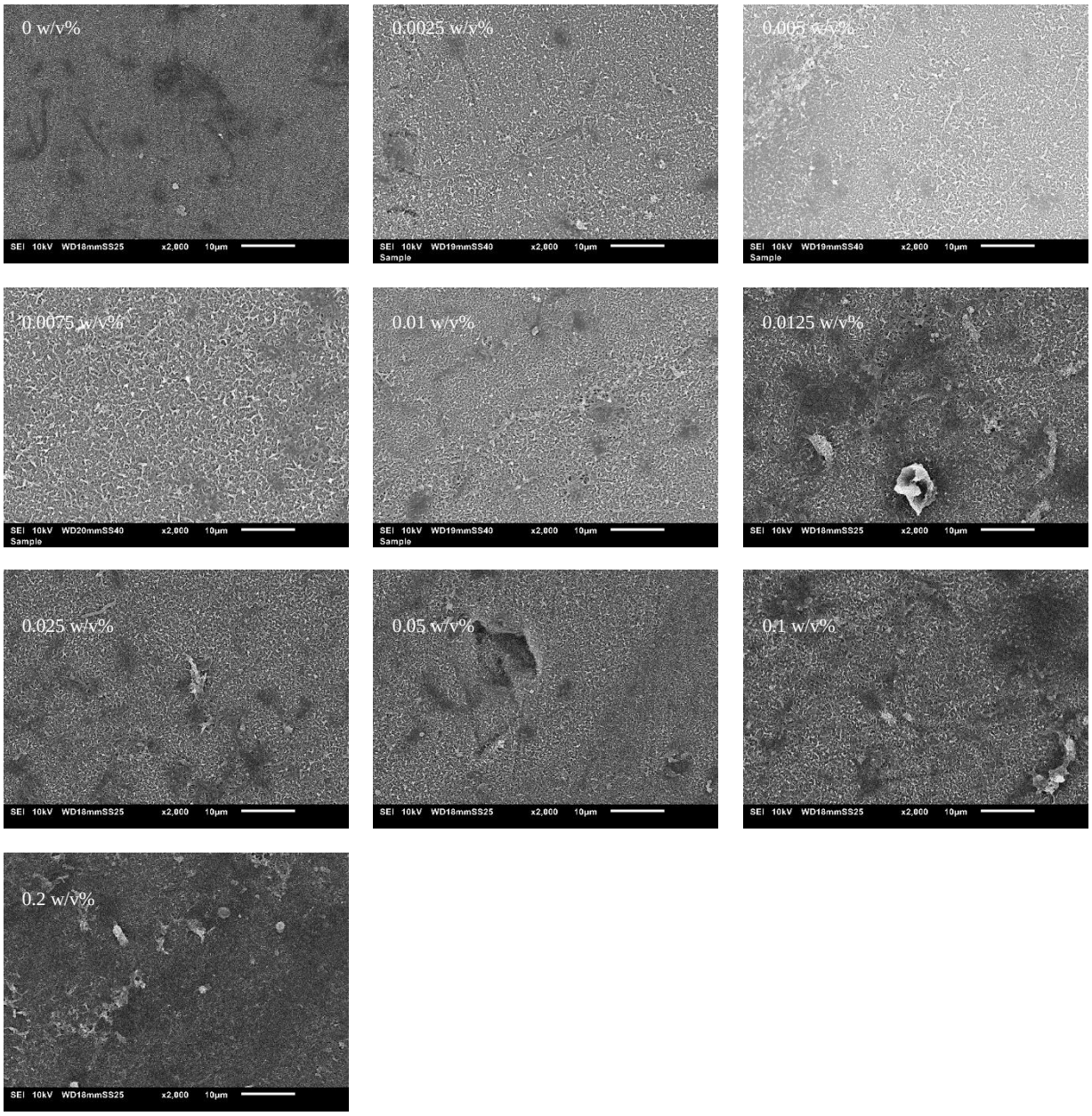

Figure S11: SEM images of the toplayer morphology of bZIF-CONV-membranes prepared with different filler concentrations in the hexane solution.

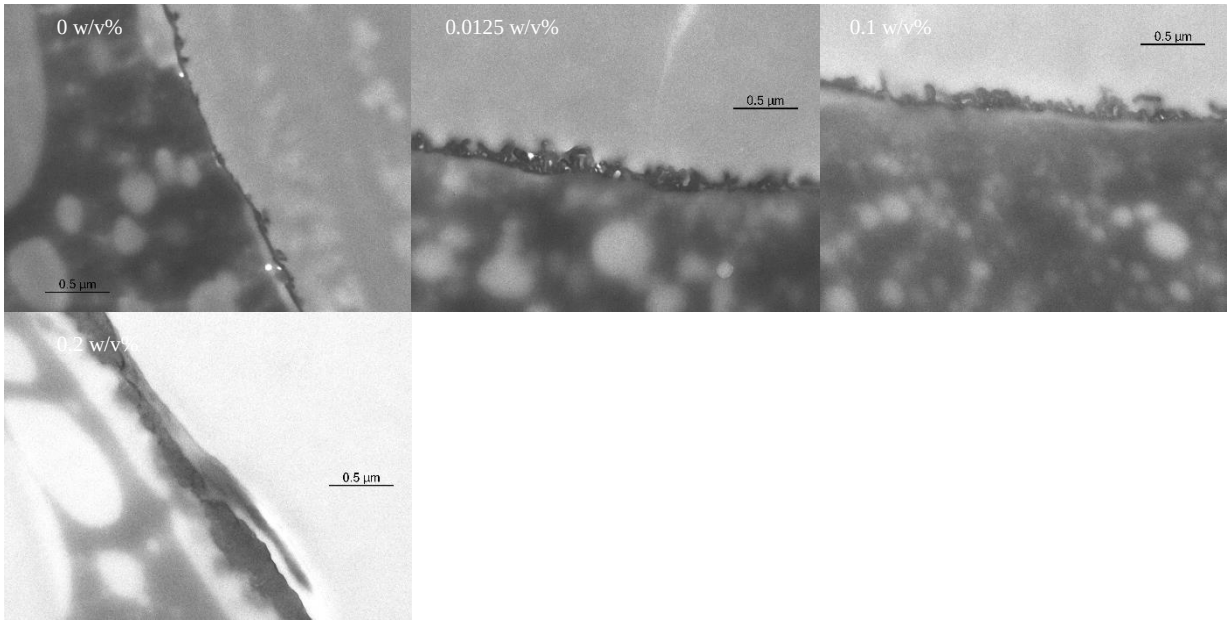

Figure S12: TEM cross-section images of bZIF-CONV-membranes prepared with different filler concentrations in the hexane solution.